Journal of Fluorescence (2020) 30:71–80
https://doi.org/10.1007/s10895-019-02471-4

ORIGINAL ARTICLE

Fluorescence of Scopoletin Including its Photoacidity and Large Stokes Shift

Hunter T. Pham [1] · Joy Yoo [1] · Michael VandenBerg [1] · Mark A. Muyskens [1]

Received: 16 September 2019 / Accepted: 12 December 2019 / Published online: 24 December 2019

Abstract

Scopoletin is highly fluorescent in water and acts as a photoacid exhibiting excited-state proton transfer, ESPT, competitive with fluorescence. Its absorbance and emission spectral characteristics yield ground-state and excited-state pK_a values of 7.4 ± 0.1 and 1.4 ± 0.1, respectively. The pK_a^* implies an ESPT rate constant an order of magnitude smaller than that for umbelliferone. This report provides quantum yield measurements in water that are comparable to quinine sulfate, and fluorescence lifetime values that are on a par with other similar coumarins yet provide insight into the ESPT process. The scopoletin anion is observed in tetrahydrofuran by reaction with a strong base. The Stokes shift of aqueous scopoletin is >100 nm in the pH range 3 to 7 due in part to its action as a photoacid. Modeling by density functional theory methods provides reasonable support for the experimental results.

Keywords Stokes shift · Photoacid · Fluorescence spectroscopy · Quantum yield · Lifetime

Introduction

Scopoletin is an important member of the simplest coumarins found in nature, that is those found in plant extracts. The most prominent of these, based on the frequency of appearing in Chemical Abstracts, have one or two substitutions involving either hydroxyl or methoxy groups in positions 6 and 7, namely umbelliferone (7-hydroxycoumarin), aesculetin (6,7-dihydroxycoumarin) and scopoletin (6-methoxy-7-hydroxycoumarin). All three of these are examples of photoacids, substances that become more acidic upon photoexcitation, the most prominently studied being umbelliferone along with 4-methylumbelliferone [1–3]. In the case of umbelliferone, the photoacidity is proposed to be a key to its antifungal properties [2]. Scopoletin has been found to be a highly fluorescent compound in water [4–8]. Goodwin and Kavanaugh [9] report that scopoletin is among the most fluorescent of the 98 coumarin aqueous solutions they surveyed, and among six selected coumarins in methanol, including umbelliferone and aesculetin, Crosby and Berthold [5] highlight the particularly intense fluorescence of scopoletin. Interest in scopoletin is also due in part to its biological activity; acting as an antioxidant [10–12], as an antidepressant [13], and as an antifungal and antibacterial agent [14]. Scopoletin is found naturally in plants often playing a role as a secondary metabolite or phytoalexin produced in response to stress. For example, Wharton et al. [15] recently reported that scopoletin is the primary, pH-dependent, fluorescent substance in aqueous extracts of wood material from the common planetree (*Platanus* × *acerifolia*).

Scopoletin in water is a weak acid in equilibrium with its anion at moderate pH. The equilibrium involving the hydroxyl proton in position 7, see Scheme 1, is characterized by the acid dissociation constant, K_a, and commonly expressed as pK_a = $-\log_{10}(K_a)$. A photoacid is a substance that has a much smaller pK_a in the first excited electronic state, pK_a^*, than in the ground state, often by more than 6 pK_a units. Figure 1 shows the fluorescence excitation and emission spectra for scopoletin at pH 5 and 9; it illustrates that while a significant shift occurs due to pH in the region where light is absorbed, the fluorescent emission remains largely unchanged. The explanation for this invariant emission is that neutral scopoletin at pH 5 absorbs light but prior to emission while in the S_1 excited state loses a

Electronic supplementary material The online version of this article (https://doi.org/10.1007/s10895-019-02471-4) contains supplementary material, which is available to authorized users.

✉ Mark A. Muyskens
mark.muyskens@calvin.edu

[1] Calvin University, 3201 Burton St SE, Grand Rapids, MI 49546, USA

Scheme 1 Scopoletin acid–base equilibrium with coumarin ring position numbering

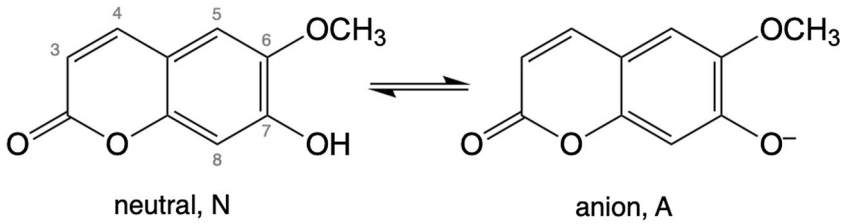

proton and fluoresces as the anion. In this model, pH 5 is below its pK_a but above the pK_a^*. The photoacid action is called photoprotolysis or excited-state proton transfer, ESPT, involving intermolecular transfer to a polar solvent molecule. If the proton loss at position 7 results in or is coordinated with proton gain at the carbonyl group, the scopoletin tautomer is formed, a process often designated excited state intramolecular proton transfer, ESIPT. If the phototautomer plays a role in the photodynamics, as it does in umbelliferone, it is typically observed as emission at longer wavelengths than the anion emission, discussed below. Figure 1 shows that scopoletin in water exhibits a large Stokes shift, the difference between the maximum emission wavelength and the maximum absorption wavelength, and when pH is below the pK_a, the photoacid effect contributes to an extraordinarily large Stokes shift. To be sure, the median Stokes shift of a representative set of commercial fluorescent dyes [16] has $\Delta\lambda = 24$ nm and $\Delta\nu$ ~1000 cm^{-1}, therefore the Stokes shift of scopoletin, $\Delta\lambda$ ~100 nm and $\Delta\nu > 6000$ cm^{-1}, can be considered remarkable.

The pK_a of the ground state can be determined by several methods related to UV-Vis absorbance spectra [17]. These methods involve monitoring a physical property, such as absorbance, that varies with pH. For this system, modeled as having two species, neutral N and anion A, a wavelength λ′ is selected where absorbance is maximally sensitive to detecting A with minimal interference by N. The A absorbance at λ′, $A(\lambda')$, then is a proxy for the ratio of the equilibrium concentrations of the two species [A]/[N]. This ratio is related to pH and pK_a by the Henderson-Hasselbalch relationship,

$$\mathrm{pH} = \mathrm{p}K_a + \log([A]/[N]) = \mathrm{p}K_a + \log(A(\lambda')).$$

This equation is inverted to give the sigmoid function,

$$A(\lambda') = 1/\left(1 + 10^{(\mathrm{p}K_a - pH)}\right),$$

where the center of the sigmoid fit of $A(\lambda')$ versus pH is equal to pK_a. This is fundamentally equivalent to the approach by several studies [18–20] yielding the pK_a for umbelliferone. In the case of scopoletin, the wavelength of the absorbance maximum can also be used as a proxy for [A]/[N]. A sigmoid fit to absorbance maximum wavelength versus pH also gives a sigmoid fit yielding a pK_a value. Both of these approaches benefit, in the case of scopoletin, from having a binary system with well-defined spectral characteristics and comparable molar absorption coefficients. Reijenga et al. discusses using fluorometric methods to determine pK_a [17]. This study adopts the wavelength maximum approach to directly observe changes yielding an experimental determination of pK_a^*.

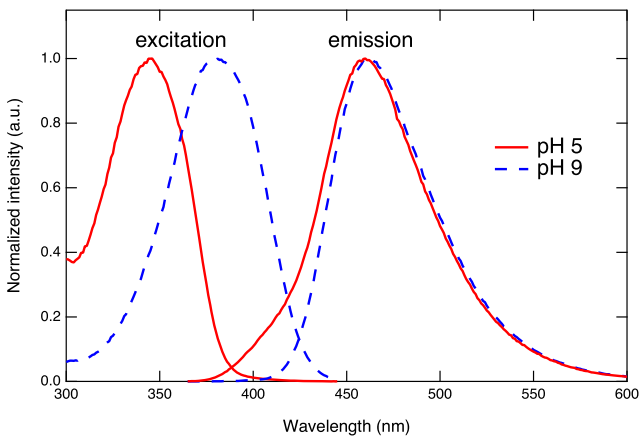

Fig. 1 Fluorescence excitation and emission spectra of scopoletin in water at pH 5 and pH 9, illustrating the photoacid behavior, and showing the extraordinary Stokes shift at pH 5

Umbelliferone is a key reference for studying the fluorescence behavior of scopoletin, which is different from umbelliferone only by the addition of a methoxy group in position 6. Umbelliferone is a weak acid with a pK_a of 7.75 [1] and exhibits a UV absorption shift from neutral to anion characterized by an isosbestic point at 337 nm [1]. For aqueous solutions with pH < pK_a, excitation of the neutral molecule results in fluorescent emission from the excited neutral near 380 nm but to a larger extent from the excited tautomer peaked at 480 nm, red-shifted by 27 nm from the peak of the 453-nm anion emission observed exclusively at pH 10 [2]. The excited state proton transfer rate constant k_{PT} is 2×10^{10} s^{-1} (lifetime of 48 ps) determined by time-resolved fluorescence [2], which is consistent with a low pK_a^* reported as ~0.4 [2]. The observed neutral emission at 380 nm is dominated by the ESPT process because it is much faster than the expected neutral fluorescence rate. Da Silva et al. [21] note that for photoacids with moderate pK_a^* (between 0 and 3), the quantity $\log_{10}(k_{PT})$ scales approximately with pK_a^*, allowing a prediction of k_{PT} from a measured pK_a^*. Conventional models for coumarin photophysics also include the cationic form, but the study by Moriya [1] shows that the umbelliferone cation only plays a significant role at pH below

0. This is consistent with the finding that the scopoletin cation is not required to play a role in the models used in this study.

Because of the priority placed on understanding structure activity relationships particularly for bioactive coumarins, substantial effort has been made to compute pK_a and pK_a^* values for coumarins. Ferrari [22] included scopoletin among the 22 coumarins studied with the aim of determining the pK_a from quantum-chemical energies, but the subset of coumarins that did not have corresponding experimental values includes scopoletin. The efforts of Jacquemin et al. [23] and Houari et al. [24] to calculate pK_a^* for selected coumarins was limited to three experimental values and did not include scopoletin. In a related study focusing on dihydroxybenzenes, Romero et al. [25] recently reported on the spectrophotometric determination of a large set of pK_a values that validated their approach to calculate pK_a. Therefore, efforts to experimentally determine photoacid properties in coumarins support the wider interest in testing computational methods to model and understand the process, and ultimately to understand potential bioactivity.

We use scopoletin absorbance and fluorescence spectra in water over a wide range of pH in order to determine the pK_a and pK_a^*, and we used the aprotic solvent tetrahydrofuran to have additional control over the loss of a proton. Quantum yield measurements quantify the high fluorescence efficiency of both the neutral and anion of scopoletin, and time-resolved fluorescence experiments provide lifetime information. Finally, we use computational modeling with the density functional theory approach to provide calculated spectra for comparison with experiment.

Materials and Methods

Scopoletin (Indofine Chemical Company, Inc., 99 + %) purity was verified by nuclear magnetic resonance spectroscopy and used without further purification. Solutions with concentrations of 17 μM were prepared using appropriate non-fluorescing and non-quenching buffers (sodium acetate, potassium dihydrogenphosphate, Tris, and sodium bicarbonate), with pH ranging from 1 to 12. The pH meter (Accumet AR15) was standardized to buffers at pH 1.67, 4.00, 7.00, and 10.00 where appropriate. Absorption and emission spectra were verified to be free of buffer and counterion effects by using solutions of near-identical pH prepared with buffers based on sodium hydroxide, nitric acid, and tetrabutylammonium hydroxide. Tetrahydrofuran (Sigma-Aldrich, 99.9 + %, HPLC grade without inhibitor) was used as an aprotic solvent to prepare a sample of 7.7 μM scopoletin. To prepare the same concentration anionic scopoletin in THF, three sodium pellets (kerosene removed by rinsing with hexanes, and pellets crushed to maximize surface area) were added to the cuvette and stirred for five minutes to ensure complete deprotonation. The anionic THF solution was stirred and analyzed over an additional two hours to verify that there was no further reaction, to the quinone, for example, or to other potential products from exposure to sodium metal. Absorption and emission spectra were collected on a *UV-Vis* spectrophotometer (Varian *Cary 100 Bio)* and spectrofluorometer (Horiba *FluoroMax-4*). Emission spectra were obtained with an excitation wavelength corresponding to the absorption peak for the first excited state, 341 and 394 nm for neutral and anionic scopoletin in THF, respectively. Excitation spectra were collected to compare to absorption spectra, and they were consistent to within 5 nm. Samples were not purged of dissolved oxygen because the presence of oxygen was observed not to have an effect on the fluorescent emission properties of scopoletin.

Quantum yield determination: A quantitative determination of the scopoletin quantum yield was carried out relative to the standard quinine sulfate (QS, 0.1 N H_2SO_4, 22 °C) [26] using 350-nm excitation for all solutions. The absolute fluorescence quantum yield of scopoletin $\Phi_S = \Phi_Q(I_S/I_Q)(A_Q/A_S)$, where Φ_Q = 0.58 for QS, $I_S/I_Q$is the ratio of the wavelength-integrated fluorescence intensity of scopoletin to quinine sulfate, A_Q/A_S is the ratio of the absorbance of scopoletin to QS at 350 nm, and the indices of refraction are assumed to be the same for all solutions. At two pH values below the pK_a and one above it, this analysis is performed over a range of absorbances from 0.02 to 0.10, giving the expected linear response of the integrated intensity. In addition, a measure of relative quantum yield across a pH range is determined by the integrated emission intensity normalized by absorbance assuming that the emission spectra are taken at the same solution concentration, excitation wavelength, excitation intensity and emission sensitivity.

Time Correlated Single Photon Counting. The instrument used to acquire the time-domain fluorescence data has been detailed elsewhere [27]. Briefly, the system uses a picosecond laser light source and time-correlated single photon counting (TSCPC) detection. The laser light source is a passively mode-locked, diode-pumped, Nd:YVO_4 laser (Spectra Physics Vanguard) that produces 13-ps pulses at a repetition rate of 80 MHz. The average power output of this laser is 2.5 W at 532 nm and 355 nm. The output of this laser is used to excite cavity dumped dye lasers synchronously (Coherent 701–3 laser equipped with 7220 cavity dumper). For the experiments reported here the excitation wavelength was 350 nm, with the dye laser operating at 700 nm (LDS698 dye, Exciton). The dye laser output (5-ps pulses, 4-MHz repetition rate) was frequency-doubled using a Type I $LiIO_3$ SHG crystal. Average power at the sample is 1 mW or less. Emission from the sample is collected with a 40x reflecting microscope objective (Ealing) and the collected light is split using a polarization-selective beam-splitter (Newport). The detection system uses two channels (vertical and horizontal polarizations), each equipped with a subtractive double monochromator (Spectral Products CM112) and a microchannel

plate-photomultiplier tube (Hamamatsu R3809u-50). The reference channel detector is a photodiode (Becker & Hickl PHD-400). The detection electronics are commercial (Becker & Hickl SPC-132), with acquisition controlled by computer code developed in-house (LabVIEW®).The instrument response function for this system is ~40 ps.

Computational Methods

All quantum chemistry calculations using density functional theory (DFT) were performed with the Gaussian 16 program package [28] and the WebMO Pro interface [29]. Full geometry optimizations of scopoletin neutral and anion in water and tetrahydrofuran were performed for the ground state using the hybrid functional B3LYP methodology [30–32] and the cc-pVTZ basis set. To represent the diffuse dielectric medium of the solvent, the default solvent cavity reaction field approach is used comprised of the polarizable continuum model (IEFPCM). Care is taken to ensure each ground state structure is at a global minimum energy, which for N involves an intramolecular hydrogen bond of the acidic proton to the oxygen at position 6. Comparison calculations using the cc-pVQZ basis set were done to check consistency of results. To model the excited state, the time-dependent DFT/B3LYP/cc-pVTZ/PCM method was used, (a) not optimizing the excited state structure to determine the S_0–S_1 transition energy corresponding to absorbance, and (b) optimizing the excited state structure to determine the S_1–S_0 transition energy corresponding to fluorescent emission.

Results and Discussion

Absorbance and Excitation Spectra with pH

Figure 2 shows the pH dependence of the absorbance spectrum of scopoletin solutions. The 10 μM concentration makes the absorbance near the isosbestic point (354 nm) around 0.1 to minimize the inner-filter effect for fluorescence spectra. A presentation of the fluorescence excitation spectra (Fig. S1) shows a second isosbestic point at 278 nm. The system has the appearance of involving a straightforward equilibrium between N at low pH shifting to A at high pH involving absorbance at longer wavelengths. Absorbance at 400 nm is maximally sensitive to the presence of A because it is near the A absorbance maximum but zero at low pH; the vertical dashed line in Fig. 2 highlights this wavelength. The left inset of Fig. 2 shows a sigmoid fit to this data that gives a pK_a of 7.48 ± 0.03. Focusing rather on the spectral shift, the right inset of Fig. 2 shows the shift in the absorbance maximum wavelength, and the sigmoid fit to this change indicates a pK_a of 7.44 ± 0.02; this second approach occurs over a narrower range of pH. These pK_a values are in good agreement with applying the same approach to the excitation intensity data (Fig. S2). Taking into account all the measures of pK_a, including the uncertainty in pH measurement, the pK_a for scopoletin is 7.4 ± 0.1. The calculated value from Ferrari [22] is 7.6, which is quite good agreement. Furthermore, Ferrari predicts scopoletin to be 0.3 pK_a units lower than umbelliferone, which also lines up well with this experimental result.

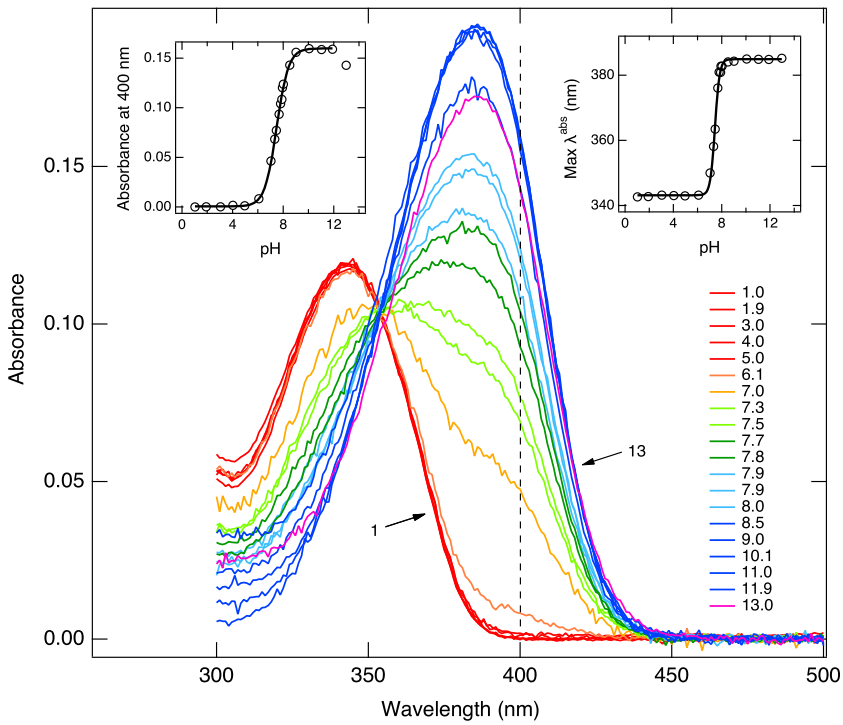

Fig. 2 Scopoletin absorbance spectra over the pH range 1 to 13 revealing an isosbestic point at 354 nm. Absorbance at 400 nm is maximally sensitive to the presence of the species absorbing at 380 nm, and the left inset shows the 400-nm absorbance as a function of pH; the solid line is a sigmoid fit to these data indicating a ground state pK_a of 7.48 ± 0.03. The right inset shows the wavelength of the absorbance maximum as a function of pH; the solid line is a sigmoid fit to these data indicating also a ground state pK_a of 7.44 ± 0.02

Emission Spectra with pH

Figure 3 shows the emission spectra from 350-nm excitation of scopoletin solutions in the pH range 1 to 13. Excitation close to the isosbestic point means absorbance is nearly constant with pH. These spectra support the model that only the electronically excited N and A are involved in the emission process because they are dominated by emission peaked at 460 nm, assigned to A, with a blue-shift at lower pH to N emission near 430. If the scopoletin tautomer emission was significant, it would show as broadening of the anion peak to the red as pH is lowered, which is where tautomer emission is observed for umbelliferone. Figure 4 shows the pH dependence of a set of normalized emission spectra in the pH region 0 to 6, with the inset showing how the emission wavelength maximum depends on pH. The emission spectrum at pH 0.5 is sufficiently below the pK_a^* to reveal that neutral scopoletin in water has an emission maximum wavelength of 434 nm. This agrees well with the 430 nm emission peak reported by Crosby and Berthold [5] in 0.1 N sulfuric acid, and with calculations discussed below. The sigmoid fit in the Fig. 4 inset is based on the spectra shown in Fig. 4 and two other experiment days. Taking into account the uncertainty in pH, the pK_a^* of scopoletin is 1.4 ± 0.1. While the work of Grzywacz and Taszner on umbelliferone [33] and aesculetin [34] present pH-dependent emission spectra analogous to Fig. 4, this study appears to be the first to apply the maximum-wavelength-sigmoid approach to experimentally determine pK_a^*. Based

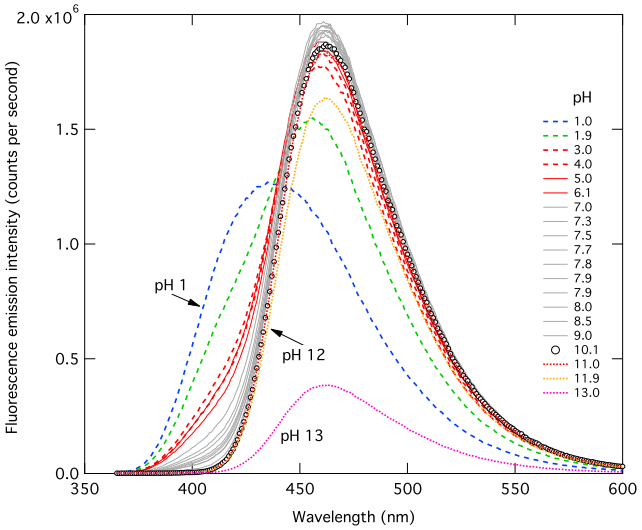

Fig. 3 Scopoletin emission spectra over the pH range 1 to 13, excitation at 350 nm (close to the isosbestic point), concentration is 10 μM in buffer. Open symbols represent the pH 10 spectrum, which is assigned to anion emission. The dashed spectra represent the low pH range and dotted spectra represent the high pH range, both show that intensity drops off at the limits of the pH range. As pH approaches the lower limit, the spectrum shifts from A emission at 460 nm to N emission at 434 nm. A key observation is the lack of any significant emission that can be assigned the tautomer, which is predicted to emit at longer wavelengths than A

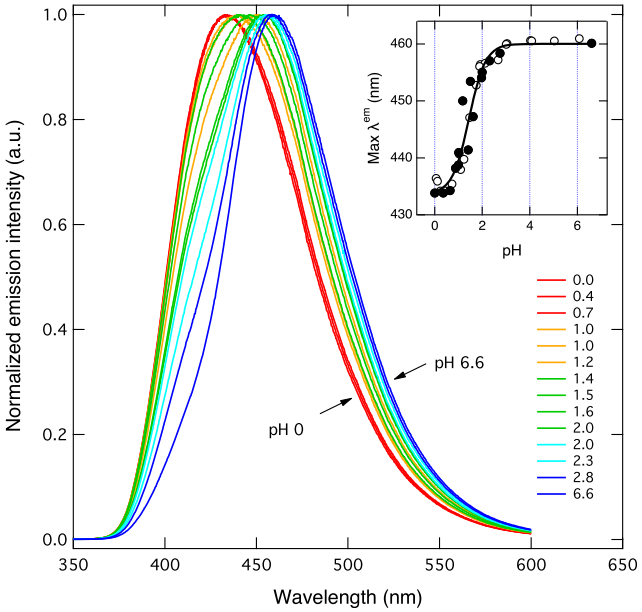

Fig. 4 Normalized emission spectra of scopoletin over the pH range 0 to 6 from excitation at 340 nm (at the peak of the N absorbance) revealing a wavelength shift from 434 nm at pH 0 to 460 nm at pH 6. The inset shows the wavelength of the emission maximum as a function of pH; the filled points are from the spectra shown in this figure, and the open points are from two other experiment days, one of which is data shown in Fig. 3 with 350-nm excitation. The solid line in the inset is a sigmoid fit to all of the inset data indicating a pK_a^* of 1.44 ± 0.06

on this study the ΔpK_a for scopoletin is 6, which is in line with several experimental ΔpK_a values reported by Houari [24]: ~7 for both umbelliferone and 4-methylumbelliferone, ~5 for 3-hydroxycoumarin. The scopoletin pK_a^* is one pK_a unit larger than that for umbelliferone, and since da Silva et al. [21] note that pK_a^* scales nearly linearly with $-\log_{10}(k_{PT})$, it suggests that the ESPT process is an order of magnitude slower in scopoletin than umbelliferone. On this basis, the scopoletin $k_{PT} = 2 \times 10^9\ s^{-1}$ (lifetime of 0.5 ns).

Fluorescence Quantum Yield

Table 1 provides quantum yield measurements relative to the standard quinine sulfate for two pHs below the pK_a and one near pH 11. These data are the result of five different determinations at each pH establishing an uncertainty of less than 10% (see Fig. S3). Typically, fluorescent simple coumarins are much more fluorescent at high pH, that is, in their A form in aqueous solution; for many examples, see Goodwin and Kavanagh [9]. An absolute quantum yield of 0.68 at pH 11 is evidence of efficient fluorescence and compares well with the umbelliferone quantum yield of 0.91 determined by Zhang [35]. At pH 6.2, absorbance will be primarily neutral scopoletin (Fig. 2b), and the quantum yield is a decrease of just 18% compared to pH 11. The relative quantum yield across the full pH range is provided by integrating the emission spectra in Fig. 3 and normalizing to the measured absorbance

Table 1 Quantum yields for scopoletin fluorescence using quinine sulfate as reference standard. Uncertainty in quantum yield is ±0.05

pH	Quantum yield
6.2	0.56
6.8	0.56
10.7	0.68

at 350 nm (shown in Fig. S4). This analysis indicates that the quantum yield at pH 6 remains constant down to pH 3 and then drops off. Above the pK_a, quantum yield appears to be roughly constant from pH 8 to 11 and drops off above 11. At pH above 12, opening of the α-pyrone ring becomes a consideration.

Time-Resolved Fluorescence

Figure 5 shows the semi-log fluorescence emission decay curves for scopoletin at pH 5 (emission from N and A) and pH 9 (emission from A). Linear fits to this data give the decay constant τ. At pH 5, N dominates in solution, and the pH-5 emission trace in Fig. 1 shows that 400-nm emission at will be primarily from N while 480-nm emission will be from A. Both pH 5 N emission (Fig. 5-trace c) and pH 9 A emission (Fig. 5-trace a) are well described by a linear fit, but pH 5 A emission (Fig. 5-trace b) clearly shows a delay before becoming linear after ~7 ns. Table 2 lists the lifetimes for the linear regions in Fig. 5 and includes results from time-resolved analysis of

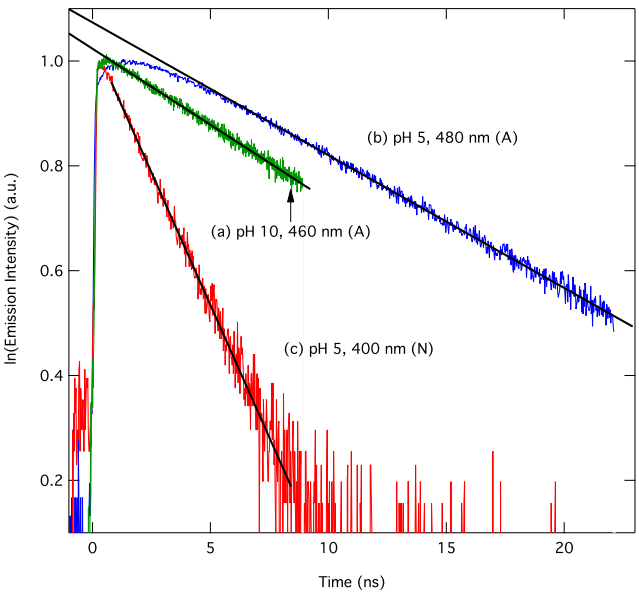

Fig. 5 Scopoletin fluorescence decay curves from TCSPC analysis, 350-nm excitation, (**a**) pH 10, 460-nm emission, monitoring A, (**b**) pH 5, 480-nm emission, monitoring A (20 nm away from wavelength maximum to minimize overlap with N emission), and (**c**) pH 5, 400-nm emission, monitoring N. Solid lines represent linear fits over selected ranges, for trace a and b the linear fit is extended beyond the fit range for comparison, residuals for the fit regions are presented in the supplemental information, Fig. S5

Table 2 Lifetime measurements τ for scopoletin fluorescence

Solvent, pH	λ_{em} (nm)	τ (ns)
Aqueous, pH 9	460	4.69 ± 0.02
Aqueous, pH 5*	480	4.76 ± 0.02
Aqueous, pH 5	400	1.41 ± 0.02
Methanol	460	2.67 ± 0.005
THF	400	0.44 ± 0.01
THF, base added	446	3.7 ± 0.1

*determined from linear region after 7.3 ns

scopoletin in methanol, tetrahydrofuran and in sodium-treated tetrahydrofuran (Fig. S6 and S7 show these decays and linear fits).

Lifetime in Aqueous Solution

The fluorescence lifetime of A at pH 9 is nearly the same as the lifetime from the linear region at pH 5. This is expected since the emission at 460 to 480 nm is dominated by A. A fluorescence lifetime of ~4.7 ns is quite reasonable for a strong fluorophore in water; for comparison, umbelliferone has an aqueous anion fluorescence lifetime of 5.2 ns [2] and coumarin 500 in methanol is 4.84 ns [36]. The obvious difference between pH-5 A and pH-9 A emission is the delay present in the pH 5 data, a decay in which ESPT is expected to play a role. The 1.4-ns radiative lifetime of pH-5 N is 3.3 times smaller than A and is expected also to be influenced by ESPT. The pH-5 N decay has the appearance of being well correlated with the delay observed in pH-5 A. The pH-5 N emission is interesting because it appears to be a single exponential based on how well it fits the linear model, and yet it is expected to be influenced by at least two processes, ESPT and fluorescence. If k_{PT} is much larger than the N fluorescence rate constant ($1/\tau_N$), then the observed emission would be determined solely by the ESPT process, as observed in umbelliferone. An ESPT process with a lifetime of 0.5 ns (predicted on the basis of pK_a^* as discussed above) is sufficiently different from what is observed that it would manifest as a double exponential. An interpretation of the pH-5 N decay involving both fluorescence and ESPT having lifetimes coincidentally similar enough to be indistinguishable is consistent with the pH-5 A emission decay and points to a k_{PT} of 7×10^8 s^{-1}, but this is at odds with the k_{PT} based on pK_a^* by a factor of 3. Nonetheless, the pH 5 data provide a direct view of the ESPT process.

Lifetime in Other Solvents

While the anion tends to dominate over a wide range of pH in aqueous solution, the scopoletin fluorescence lifetime in methanol and tetrahydrofuran is expected to be due to N

emission because the ESPT process is predicted to be too slow even in methanol to compete with fluorescence [2]. Table 3 presents a comparison of the methanol N lifetime τ_N to the aqueous A lifetime τ_A for scopoletin, umbelliferone, and 4-methylumbelliferone. In each case, τ_N is smaller than τ_A, although scopoletin stands out as having the largest τ_N of the three. The lifetime of scopoletin emission in tetrahydrofuran with base added, assuming N is completely converted to A, is comparable to the aqueous A lifetime by a factor of 0.8 (τ_{THF}/τ_{H_2O}). The lifetime of scopoletin in tetrahydrofuran without base added represents N emission, which is a factor of 0.12 smaller than the THF-A lifetime, a factor quite similar to that for umbelliferone in Table 3.

Spectra in Tetrahydrofuran

Figure 6 shows the normalized, absorbance and fluorescence emission spectra for scopoletin in the aprotic solvent THF for the neutral and anionic forms. Both N spectra agree well with those observed by Smith et al. [6]. The A spectra in Fig. 6 reveal that both absorbance and emission are red shifted upon removing a proton, similar to what is observed in water. The un-normalized A emission intensity is considerably larger than N emission. The ratio of the integrated, un-normalized, emission curves, corrected for differences in absorbance and excitation lamp intensity at the excitation wavelengths, gives a relative quantum yield (Φ_A/Φ_N) of 10 ± 1. Similar to water, A is the stronger fluorophore, but in water the quantum yield ratio is only 1.2.

Stokes Shift

Table 4 summarizes the spectral characteristics of scopoletin for several pH values and for the neutral and anion forms in THF. Comparing the aqueous spectra to the THF results, there is a small 3-nm blue shift in N absorbance from the aqueous spectrum to that for THF. Abu-Eittah and El-Tawil [4] also observe a similar solvent effect with scopoletin, a modest blue shift in the N absorbance spectrum going from ethanol to the less polar dioxane, and they note a similar blue shift for aesculetin in the same solvents. Nad and Pal [36] observed a 10-nm blue shift in absorbance of coumarin 500 (an ionizable proton on the ethyl-amino group in position 7) by a decrease in solvent polarity (polar methanol to less polar ethyl acetate). DFT/PCM models comparing scopoletin in water and THF also predict a blue shift for N absorbance but it is small, less than 1 nm. For the A absorbance wavelength, there is observed a red shift from water to THF, and the calculation also predicts a small red shift. Table 4 also lists the Stokes shift for each case. Crosby [5] noted the large Stokes shifts in the most prominent natural coumarins, umbelliferone, aesculetin, and scopoletin, but it is worth pointing out that the Crosby account, which only compared emission at pH 1 and 10, misses that fact that the Stokes shift for scopoletin over the pH range 3 to 7 is >110 nm due to the photoacid effect.

Computational Modeling

Table 4 also includes the calculated absorbance and emission wavelengths for comparison with experiment. Despite the fact that the model always underestimates the wavelengths for both absorption and emission, the shift from neutral to anion and from one solvent to another is encouraging. The predicted wavelengths are all within 10% and most are within 5% of the experimental value. Another measure of the relative success of the modeling is the prediction of absorbance ratio of anion to neutral. In water, the absorbance maximum of the anion is 1.64 times larger than that for the neutral (visible in Fig. 2). The model provides intensities for the absorption transition, and the model ratio of anion to neutral is 1.69. In THF there is a similar anion to neutral intensity ratio for both experiment and model, 1.45 and 1.67, respectively. So, both the wavelength and relative intensities of the model are in reasonable agreement with experiment, supporting the notion that the B3LYP/cc-pVTZ/PCM level of theory does a reasonable job of modeling scopoletin. In terms of the calculated Stokes shift expressed in nm units (for example, $\lambda_A^{em}-\lambda_A^{abs}$), the value is always underestimated, and the average difference with experiment is 21%, with the largest different at 30%; and yet the modeling is able to get the right trend from largest to smallest Stokes shift. For the extraordinary Stokes shift at pH 5, the calculated result requires imposing the photoacid behavior ($\lambda_A^{em}-\lambda_N^{abs}$) to calculate a Stokes shift of about 100 nm (14% shy of the experimental value).

Modeling the tautomer at the same level of theory predicts that tautomer emission will be longer than the anion by ~40 nm.

Table 3 Lifetime comparisons among three coumarins

Coumarin	τ_N (methanol) (ns)	τ_A (water) (ns)	τ_N/τ_A	Citation
scopoletin	2.7	4.7	0.57	this work
umbelliferone	0.7	5.2	0.16	[3]
4-methylumbelliferone	1.2	5.1	0.24	[3]

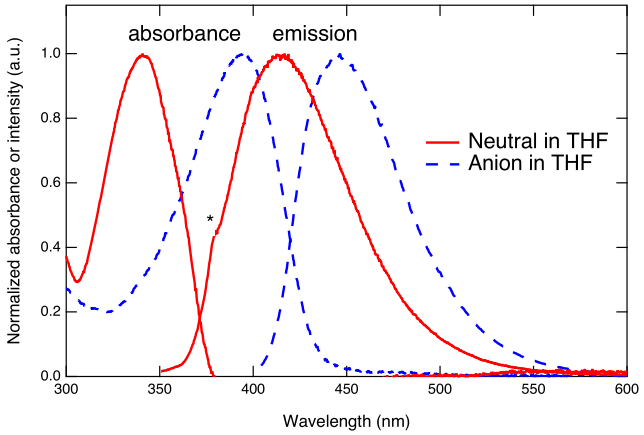

Fig. 6 Normalized absorbance and fluorescence emission spectra of neutral and anionic 7.7 μM scopoletin in tetrahydrofuran. N is converted completely to A by the addition of sodium to the solution. Excitation is at the N and A absorbance maxima, 341 and 393 nm, respectively. The fact that the water Raman signal is visible in the N spectrum, labeled with the *, is an indication that integrated, unnormalized, neutral emission spectrum is 17 times smaller than the anion emission

A graphical representation is included in Fig. S8. This difference between A and T is similar to what is observed experimentally for the umbelliferone tautomer. The experimental aqueous emission spectra presented here lack significant change in intensity with pH in this region, which suggests that the tautomer does not play a significant role in the photodynamics in scopoletin.

Conclusions

This study has contributed several photophysical properties to the description of scopoletin fluorescence. Its behavior as a photoacid helps explain its remarkably large Stoke shift. The pH-dependent absorbance and emission spectra allow us to determine the ground-state and excited-state pK_a to be 7.4 ± 0.1 and 1.4 ± 0.1, respectively. The pK_a^* implies an ESPT rate constant an order of magnitude smaller than that for umbelliferone. The spectra also suggest that the photodynamics involves the neutral and anion with little to no participation of the tautomer. Our current interest in applying a similar experimental approach to aesculetin offers the prospect of comparison with scopoletin, as both coumarins have oxygen substitution in the same two benzene ring locations. The addition of more experimental pK_a values will permit the testing of our ability to calculate pK_a and pK_a^* for coumarin structures. Since Simkovitch et al. [2] have described the direct connection of umbelliferone photoacidity to its antifungal activity, it will be interesting for those focused on coumarin bioactivity to test whether similar structure-function relationships extend to scopoletin and other photoacidic coumarins, like aesculetin. The measured scopoletin quantum yield is consistent with it having a bright, striking emission, and the fluorescence lifetime of scopoletin is similar to other highly fluorescent coumarins. The fact that the quantum yield remains high at low pH may make it more useful than umbelliferone as a fluorescent indicator, although this study shows that the absorbance and emission vary with pH over quite different ranges. Finally, modeling with

Table 4 Observed and calculated (in italics) excitation and emission wavelength maxima and the Stokes shift for scopoletin; solution concentration for experimental results are 10 μM and 7.7 μM in water and tetrahydrofuran, respectively

Solvent, pH		λ^{ex}, nm	λ^{em}, nm	Stokes shift (nm)	Stokes shift (cm^{-1})
Water, 0.2	Experiment	344	434	90	6030
	Calculation	*334*	*397*	*63*	*4750*
	Difference*	10, 3%	34, 8%	27, 30%	1300, 20%
Water, 5.0	Exp.	346	460	114	7200
	Calc.	–	–	*98†*	*6800*
	Diff.	–	–	16, 14%	400, 5%
Water, 9.0	Exp.	380	461	81	4600
	Calc.	*375*	*432*	*57*	*3500*
	Diff.	5, 1.3%	29, 6%	24, 30%	1100, 24%
THF	Exp.	341	417	76	5300
	Calc.	*334*	*392*	*58*	*4400*
	Diff.	7, 2%	25, 6%	18, 24%	900, 17%
THF, base added	Exp.	394	446	52	2960
	Calc.	*378*	*427*	*49*	*3040*
	Diff.	16, 4%	19, 4%	3, 6%	−80, 3%

*difference between experimental and calculated value, expressed as absolute difference and percent difference from experimental value

† assuming the photoacid model $\lambda_A^{em} - \lambda_N^{abs}$

the B3LYP/cc-pVTZ/PCM method gives a reasonable description of the absorbance and emission characteristics.

Acknowledgements The authors are grateful for the following fellowships that supported people who worked on this project: the Thedford P. Dirkse Summer Research Fellowship (HP, MVB) and the Rollin M. Gerstacker Foundation Student Research Fellowship (JY). We thank Prof. Gary Blanchard (Michigan State University) for his generous provision of access to the TCSPC system. The computational modeling is supported by National Science Foundation (MRI-grant 1726260). The authors thank Drs. Chad Tatko, Michael Barbachyn, and Carolyn Anderson, for their helpful guidance; and Yukun Tu and Daniel Harmon for their assistance in the research lab.

Compliance with Ethical Standards

Competing Interests The authors declare no competing financial interest.

References

1. Moriya T (1983) Excited-state reactions of coumarins in aqueous solutions. I. The phototautomerization of 7-Hydroxycoumarin and its derivative. BCSJ 56:6–14. https://doi.org/10.1246/bcsj.56.6
2. Simkovitch R, Huppert D (2015) Photoprotolytic processes of Umbelliferone and proposed function in resistance to fungal infection. J Phys Chem B 119:14683–14696. https://doi.org/10.1021/acs.jpcb.5b08439
3. Simkovitch R, Pinto da Silva L, Esteves da Silva JCG, Huppert D (2016) Comparison of the photoprotolytic processes of three 7-Hydroxycoumarins. J Phys Chem B 120:10297–10310. https://doi.org/10.1021/acs.jpcb.6b01383
4. Abu-Eittah RH, El-Tawil BAH (1985) The electronic absorption spectra of some coumarins. A molecular orbital treatment. Can J Chem 63:1173–1179. https://doi.org/10.1139/v85-200
5. Crosby DG, Berthold RV (1962) Fluorescence spectra of some simple coumarins. Anal Biochem 4:349–357. https://doi.org/10.1016/0003-2697(62)90136-7
6. Smith GJ, Dunford CL, Roberts PB (2010) The photostability and fluorescence of hydroxycoumarins in aprotic solvents. J Photochem Photobiol A Chem 210:31–35. https://doi.org/10.1016/j.jphotochem.2009.12.009
7. Smith GJ, Weston RJ, Tang Y et al (2012) Photoproducts of 7-Hydroxycoumarins in aqueous solution. Aust J Chem 65:1451–1456. https://doi.org/10.1071/CH12292
8. Nahata A, Dixit VK (2008) Spectrofluorimetric estimation of Scopoletin in Evolvulus alsinoides Linn. And Convulvulus pluricaulis Choisy. Indian J Pharm Sci 70:834–837. https://doi.org/10.4103/0250-474X.49139
9. Goodwin RH, Kavanagh F (1950) Fluorescence of coumarin derivatives as a function of pH. Arch Biochem 27:152–173
10. Kostova I, Bhatia S, Grigorov P et al (2011) Coumarins as antioxidants. Curr Med Chem 18:3929–3951
11. Vianna DR, Bubols G, Meirelles G et al (2012) Evaluation of the antioxidant capacity of synthesized coumarins. Int J Mol Sci 13:7260–7270. https://doi.org/10.3390/ijms13067260
12. Malik A, Kushnoor A, Saini V et al (2011) In vitro antioxidant properties of Scopoletin. J Chem Pharm Res 3:659–665
13. Capra JC, Cunha MP, Machado DG et al (2010) Antidepressant-like effect of scopoletin, a coumarin isolated from Polygala sabulosa (Polygalaceae) in mice: evidence for the involvement of monoaminergic systems. Eur J Pharmacol 643:232–238. https://doi.org/10.1016/j.ejphar.2010.06.043
14. Gnonlonfin GJB, Sanni A, Brimer L (2012) Review Scopoletin - a coumarin phytoalexin with medicinal properties. Crit Rev Plant Sci 31:47–56. https://doi.org/10.1080/07352689.2011.616039
15. Wharton J, Izaguirre I, Surdock A et al (2018) Hands-on demonstration of natural substance fluorescence in simple tree extracts: sycamore. J Chem Educ 95:615–619. https://doi.org/10.1021/acs.jchemed.7b00611
16. Gao Z, Hao Y, Zheng M, Chen Y (2017) A fluorescent dye with large stokes shift and high stability: synthesis and application to live cell imaging. RSC Adv 7:7604–7609. https://doi.org/10.1039/C6RA27547H
17. Reijenga J, van Hoof A, van Loon A, Teunissen B (2013) Development of methods for the determination of pKa values. Anal Chem Insights 8:53–71. https://doi.org/10.4137/ACI.S12304
18. Fink DW, Koehler WR (1970) pH effects on fluorescence of umbelliferone. Anal Chem 42:990–993. https://doi.org/10.1021/ac60291a034
19. Grzywacz J, Taszner S, Kruszewski J (1978) Further study on the forms of Umbelliferone in excited state. Zeitschrift für Naturforschung A 33:1307–1311. https://doi.org/10.1515/zna-1978-1108
20. Mattoo BN (1958) Dissociation constants of hydroxy coumarins. Trans Faraday Soc 54:19–24. https://doi.org/10.1039/TF9585400019
21. Pinto da Silva L, Simkovitch R, Huppert D, Esteves da Silva JCG (2017) Combined experimental and theoretical study of the photochemistry of 4- and 3-hydroxycoumarin. J Photochem Photobiol A Chem 338:23–36. https://doi.org/10.1016/j.jphotochem.2017.01.032
22. Ferrari AM, Sgobba M, Gamberini MC, Rastelli G (2007) Relationship between quantum-chemical descriptors of proton dissociation and experimental acidity constants of various hydroxylated coumarins. Identification of the biologically active species for xanthine oxidase inhibition. European Journal of Medicinal Chemistry 42:1028–1031. https://doi.org/10.1016/j.ejmech.2006.12.023
23. Jacquemin D, Perpète EA, Ciofini I, Adamo C (2008) Fast and reliable theoretical determination of pKa* for photoacids. J Phys Chem A 112:794–796. https://doi.org/10.1021/jp7105814
24. Houari Y, Jacquemin D, Laurent AD (2013) TD-DFT study of the pKa∗ for coumarins. Chem Phys Lett 583:218–221. https://doi.org/10.1016/j.cplett.2013.08.002
25. Romero R, Salgado PR, Soto C et al (2018) An experimental validated computational method for pKa determination of substituted 1,2-Dihydroxybenzenes. Front Chem 6. https://doi.org/10.3389/fchem.2018.00208
26. Lakowicz JR (2006) Principles of fluorescence spectroscopy, 3rd ed. Springer US
27. Pillman HA, Blanchard GJ (2010) Effects of ethanol on the organization of phosphocholine lipid bilayers. J Phys Chem B 114:3840–3846. https://doi.org/10.1021/jp910897t
28. Frisch MJ, Trucks GW, Schlegel HB, et al Gaussian 16 Revision B.01
29. Schmidt J, Polik W WebMO pro. WebMO, LLC, Holland, MI, USA. Available from http://www.webmo.net
30. Becke AD (1988) Density-functional exchange-energy approximation with correct asymptotic behavior. Phys Rev A 38:3098. https://doi.org/10.1103/PhysRevA.38.3098
31. Becke AD (1993) Density-functional thermochemistry. III. The role of exact exchange. J Chem Phys 98:5648. https://doi.org/10.1063/1.464913
32. Lee C, Yang W, Parr RG (1988) Development of the Colle-Salvetti correlation-energy formula into a functional of the electron density. Phys Rev B 37:785. https://doi.org/10.1103/PhysRevB.37.785

33. Grzywacz J, Taszner S (1977) Ionic forms of umbelliferone. B ACAD POL SCI SMAP 25:447–453
34. Grzywacz J, Taszner S (1982) Influence of pH on the absorption and fluorescence spectra of 6,7-Dihydroxycoumarin in aqueous solution. Zeitschrift für Naturforschung A 37:262–265. https://doi.org/10.1515/zna-1982-0311
35. Zhang J, Liu C, Wei Y (2011) Fluorescence quantum yield and ionization constant of umbelliferone. Chemistry Bulletin / Huaxue Tongbao 74:957–960
36. Nad S, Pal H (2003) Photophysical properties of Coumarin-500 (C500): unusual behavior in nonpolar solvents. J Phys Chem A 107:501–507. https://doi.org/10.1021/jp0211411